NBS MONOGRAPH 46

Analysis of Coaxial Two-Terminal Conical Capacitor

U.S. DEPARTMENT OF COMMERCE
NATIONAL BUREAU OF STANDARDS

THE NATIONAL BUREAU OF STANDARDS

Functions and Activities

The functions of the National Bureau of Standards are set forth in the Act of Congress, March 3, 1901, as amended by Congress in Public Law 619, 1950. These include the development and maintenance of the national standards of measurement and the provision of means and methods for making measurements consistent with these standards; the determination of physical constants and properties of materials; the development of methods and instruments for testing materials, devices, and structures; advisory services to government agencies on scientific and technical problems; invention and development of devices to serve special needs of the Government; and the development of standard practices, codes, and specifications. The work includes basic and applied research, development, engineering, instrumentation, testing, evaluation, calibration services, and various consultation and information services. Research projects are also performed for other government agencies when the work relates to and supplements the basic program of the Bureau or when the Bureau's unique competence is required. The scope of activities is suggested by the listing of divisions and sections on the inside of the back cover.

Publications

The results of the Bureau's research are published either in the Bureau's own series of publications or in the journals of professional and scientific societies. The Bureau itself publishes three periodicals available from the Government Printing Office: The Journal of Research, published in four separate sections, presents complete scientific and technical papers; the Technical News Bulletin presents summary and preliminary reports on work in progress; and Basic Radio Propagation Predictions provides data for determining the best frequencies to use for radio communications throughout the world. There are also five series of nonperiodical publications: Monographs, Applied Mathematics Series, Handbooks, Miscellaneous Publications, and Technical Notes.

A complete listing of the Bureau's publications can be found in National Bureau of Standards Circular 460, Publications of the National Bureau of Standards, 1901 to June 1947 ($1.25), and the Supplement to National Bureau of Standards Circular 460, July 1947 to June 1957 ($1.50), and Miscellaneous Publication 240, July 1957 to June 1960 (Includes Titles of Papers Published in Outside Journals 1950 to 1959) ($2.25); available from the Superintendent of Documents, Government Printing Office, Washington, D.C.

UNITED STATES DEPARTMENT OF COMMERCE • Luther H. Hodges, *Secretary*
NATIONAL BUREAU OF STANDARDS • A. V. Astin, *Director*

Analysis of Coaxial Two-Terminal Conical Capacitor

M. C. Selby

National Bureau of Standards Monograph 46

Issued April 6, 1962

For sale by the Superintendent of Documents, U.S. Government Printing Office
Washington 25, D.C. - Price 20 cents

Contents

Analysis of Coaxial Two-Terminal Conical Capacitor

M. C. Selby

Adjustable capacitors having electrodes in the form of coaxial cones or frustums have been used on rare occasions in the past; but their potential superiority to other types of capacitors for some important applications have been overlooked. The advantage of this geometry over cylindrical or disk forms is that the practical capacitance range is several times larger. An example cites the capacitance ranges of a disk, cylindrical, and conical type to be 10, 40, and 168 to one, respectively. An approximate equation was derived for this conical capacitor and close agreement is shown between computed and measured values of capacitance versus electrode displacement. Multiple cone and different shape electrodes are suggested to obtain large values of capacitance with an appreciable saving of space and further increased range of capacitance. The electric field is plotted and its construction steps for axial symmetry are given.

1. Introduction

Adjustable two-terminal capacitors of coaxial form are frequently more suitable for a given application than the conventional rotary or compression types [1][1]. Variation of capacitance in the former is obtained by relative linear displacement of one electrode, usually a cylinder or a disk, with respect to another similar stationary electrode. Unfortunately, cylindrical and disk electrodes have a relatively limited capacity range.

Let us assume a certain given cylindrical space within which an adjustable capacitor with a maximum practical capacitance range is to be placed. End and shielding effects are assumed negligible. Capacitance values with a reproducibility of the order of 0.2 of a percent or better are to be available throughout the entire range.

Conical electrodes are intuitively attractive because they represent an intermediate case between cylindrical and disk electrodes. For coaxial cylinders, capacitance is directly proportional to the length of the meshed sections if end effects are neglected. Thus if the available travel is 2 in. and 0.05 in. is the minimum displacement that can be reproduced to 0.2 percent, the available capacitance range is about 40 to 1. On the other hand, for practical purposes, two parallel, equal-diameter disk electrodes, placed inside a tube of approximately the same diameter, cease to respond to the capacitive law alone when their separation exceeds approximately one radius of the disks; at these distances the effects of the TM_{01} mode induced by the high-voltage electrode inside the tube become increasingly noticeable. Since we are interested in the purely capacitive range we see that, for the example cited, and for 1-in. disks, the range would be approximately 10:1. It is shown below that with conical electrodes one can realize a range many times that of a cylindrical or disk capacitor.

2. Conical Capacitor

Consider a capacitor formed by two right conductive frustums, as shown in figures 1 and 2. The cross section in figure 2 shows the essential dimensional elements of this capacitor. Let the sections of the conical-electrode surfaces, indicated by the length l in figure 2, be referred to as the "meshed" surfaces. Let also:

2θ=angle of the cones

D=adjustable distance between the apexes of the cones. As D increases, the capacity decreases because the distances between the conical surfaces increase and the length of meshed surfaces is reduced.

h=the height of the inside cone (A) from its apex to the base of its effective meshed surface.

[1] Figures in brackets indicate the literature references at the end of this Monograph.

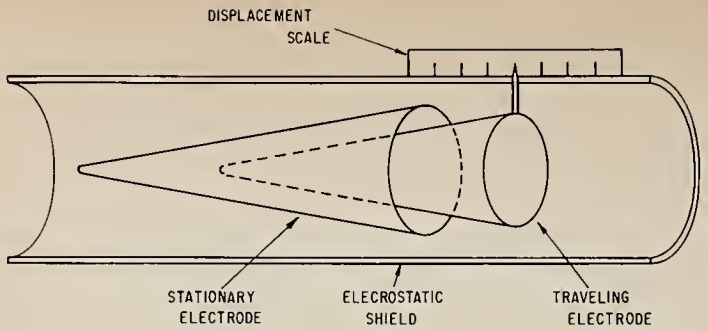

FIGURE 1. *Right-cone continuously adjustable capacitor.*

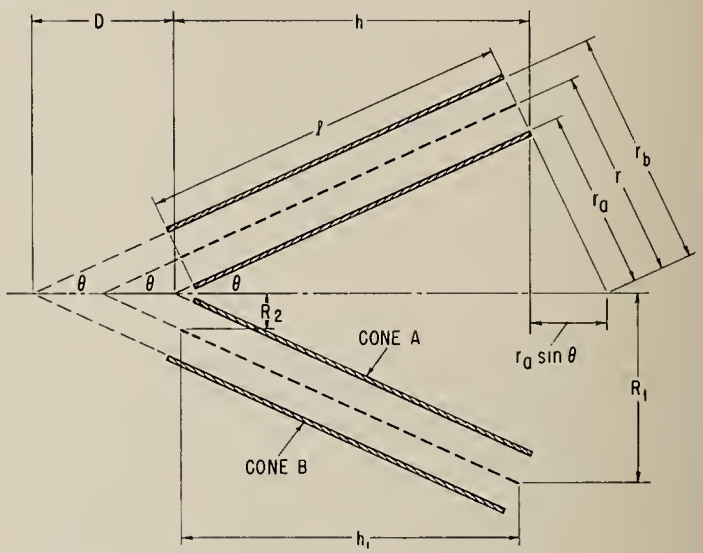

FIGURE 2. *Cross-sectional dimensions of conical capacitor.*

Solid lines indicate the conducting surfaces of frustums A and B respectively. Heavy dashed lines indicate a surface of a frustum taken at random parallel to the two conducting surfaces. The thin dashed lines indicate the geometric extention of the 3 surfaces to the apexes of the cones.

The electrostatic shield, shown in figure 1, is normally grounded and either electrode, male or female, may be connected to it. Connection of the male to the shield is particularly advisable when measurement of capacitance increments of this capacitor is to be done: this eliminates interfering varying capacitance of the male electrode to ground. This is discussed further in appendix V.

The problem is to determine the capacitance of this type of construction. A rigorous analytical solution seems unfortunately unobtainable at this time. The application of standard mathematical techniques did not yield a rigorous solution (see appendix VI).

In arriving at any mathematical expression of capacitance, the following steps are generally involved:

(a) Determination of the potential distribution within the spaces occupied by the electrodes for given surface potentials of the electrodes,

(b) determination of potential gradients at the desired electrode surfaces,

(c) determination of charge distribution and of the total charge (by integration) on the electrode in question, and

(d) determination of the capacitance between the given electrode and its surroundings from the known charge and the surface potentials.

The approximate approach given below yields satisfactory agreement with experimental results for the application at hand. In order to develop more confidence in the approximate solution, one of the field construction methods, the graphical, was partly employed to justify introductory assumptions; the steps are given in appendixes III and IV. Appendix III discusses the field construction and principles involved, and IV discusses the justification of the basic assumptions used for the approximate solution. Experimental results obtained from construction and measurements are given further in the text.

Figure 3 [2] shows the electrostatic field and potential distribution in a plane passing through the axis and any base diameter of the cones; the lines of force between the meshed surfaces are everywhere essentially straight except for a relatively small fringing flux region at

[2] See appendix III for method of construction and meaning of symbols.

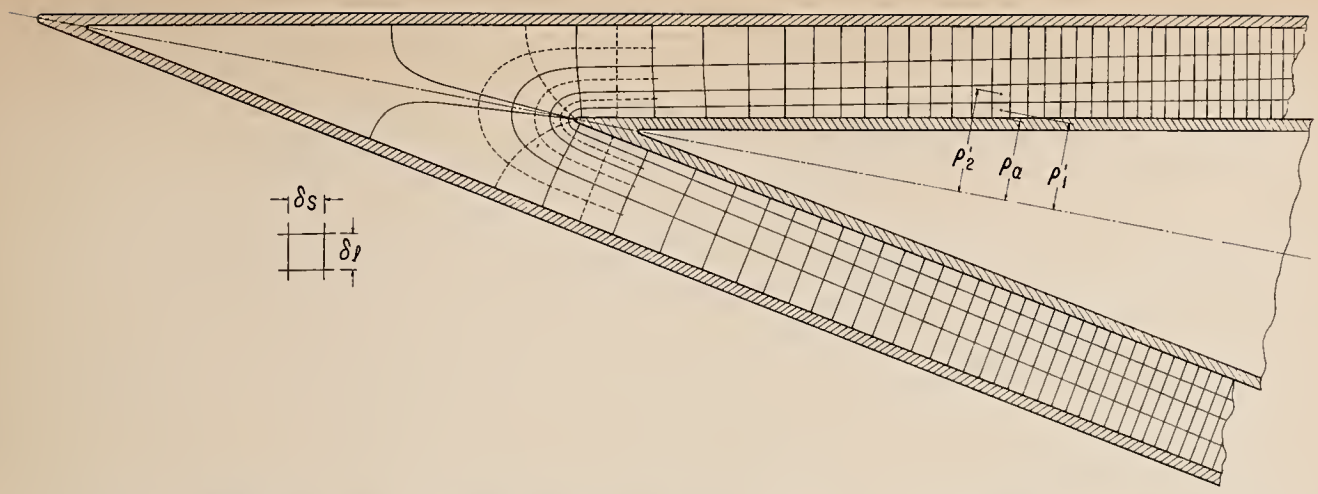

FIGURE 3. *Electric field map in a homogeneous isotropic dielectric of a coaxial parallel-cone capacitor.*

the ends of the frustums; the latter region becomes more negligible as the spacing between the electrodes decreases and as the ratio of the height of the frustums to this spacing increases. It should be clearly understood that the actual limit on the maximum spacing for which the approximation holds will have to be determined by measurements and agreement with an analytical expression to the accuracy desired. One may notice in figure 3 a slight departure of the equipotential surfaces from parallelism with the electrodes and with each other; that this may be neglected in the present problem is shown in appendix IV. The potential gradient is therefore perpendicular to the two metal surfaces nearly everywhere in the space between them. Since the conical conducting surfaces are parallel and coaxial, it follows that the lines of force in the dielectric space (assumed to be air) are everywhere normal to both surfaces. Moreover, since the electrodes are equipotential surfaces, it follows also that everywhere over these surfaces and over any other surface parallel to and located between these conducting surfaces

$$\mathbf{E}\cdot\boldsymbol{\eta}=E=-\frac{dv}{dn}=\text{constant} \tag{1}$$

where $\mathbf{E}$ is the potential gradient or the electric field intensity and $\boldsymbol{\eta}$ is unit vector normal to the surfaces. One may show the above to be true as follows [2].

Any surface parallel to and located between the two parallel conical conducting surfaces is an equipotential surface. $\mathbf{E}$ is constant over any one of these surfaces because for any given increment, Δn, along the normal from a given equipotential surface there will be the same increment, Δv, at all points of this surface to another equipotential surface. Thus equation (1) holds as long as the electrostatic lines are essentially straight. For the same reason $\mathbf{E}$ is constant over either one of the two conducting surfaces as well. But

$$\mathbf{E}\cdot\boldsymbol{\eta}=K\sigma \tag{2}$$

where σ is the surface charge density and K is a constant. Therefore, σ is constant over the surface of either conductor, and the flux-line density which is proportional to σ is also constant over any of the equipotential surfaces. In reality σ is never precisely constant over the conductor surfaces; it is a maximum at the apex of the inside cone and a minimum at the apex of the inside conical surface of the outer cone; the nonuniformity of σ is more pronounced for wide spacings between the conductors.

Referring to figure 2 and taking the surface, S_f, of any other coaxial frustum of half-angle, θ, located between the two conical electrodes and applying Gauss law to this surface, we have

$$\int_S \mathbf{D}\cdot d\mathbf{S}=\epsilon E S_f=Q. \tag{3}$$

The dielectric constant of the interelectrode space is ϵ and the integral is applied only to the conical surface above because the surfaces of the bases of the frustum by assumption do not contribute any electric flux.

The surface of the frustum of altitude h_1 and base radii R_1 and R_2 is

$$S_f=\pi(R_1+R_2)\sqrt{h_1^2+(R_1-R_2)^2}. \tag{4}$$

In order to express capacitance values in terms of D and h, we have from the geometry of the figure:

$$R_1=r\cos\theta \tag{5}$$

$$h_1=l\cos\theta \tag{6}$$

$$R_2=r\cos\theta-l\sin\theta \tag{7}$$

and

$$S_f=\pi(2r\cos\theta-l\sin\theta)\sqrt{l^2\cos^2\theta+l^2\sin^2\theta}$$

$$=\pi l(2r\cos\theta-l\sin\theta) \tag{8}$$

where r is the length of the normal from the axis to this surface at its larger base and l is the length of the meshed conical surfaces.

Substituting into equation (3)

$$Q=\epsilon\pi lE(2r\cos\theta-l\sin\theta)$$

and

$$E=Q/[\epsilon\pi l(2r\cos\theta-l\sin\theta)]. \tag{9}$$

Because of conical symmetry, the potential at the surface of this frustum, as well as of all others, depends only on r; therefore, the potential difference, V, between frustum A and B is

$$V=-\int_{r_b}^{r_a}Edr=-\frac{Q}{\epsilon\pi l}\int_{r_b}^{r_a}\frac{dr}{(2r\cos\theta-l\sin\theta)}=\frac{-Q}{2\epsilon\pi l\cos\theta}\ln(2r\cos\theta-l\sin\theta)\Big|_{r_b}^{r_a} \tag{10}$$

$$V=\frac{Q}{2\epsilon\pi l\cos\theta}\ln\frac{(2r_b\cos\theta-l\sin\theta)}{(2r_a\cos\theta-l\sin\theta)}. \tag{11}$$

Rearranging to obtain the capacitance we have

$$C=\frac{Q}{V}=\frac{2\pi\epsilon l\cos\theta}{\ln\dfrac{2r_b\cos\theta-l\sin\theta}{2r_a\cos\theta-l\sin\theta}}. \tag{12}$$

Expressing r_a and r_b in terms of h and D (see appendix I), we have

$$C=\frac{2\pi\epsilon l\cos\theta}{\ln\left[1+\dfrac{2D\cos^2\theta}{2h-l\cos\theta}\right]}. \tag{13}$$

When the internal electrode is a cone, it may be considered a frustum having a negligibly small top section and an altitude $h=l\cos\theta$. Then

$$C=\frac{2\pi\epsilon h}{\ln[1+2(D/h)\cos^2\theta]}. \tag{14}$$

Using the rationalized MKS units, h is in meters (both D and h in the logarithmic term may be expressed in any identical units), and $\epsilon\cong 8.854\times10^{-12}$ farads per meter (in vacuum and approximately in air) and

$$C=55.6h\frac{1}{\ln[1+2(D/h)\cos^2\theta]}\text{ picofarads.} \tag{15}$$

3. Computed and Measured Values

Figure 4 compares experimental data with calculations based on eq (15). $\theta=10°34'$, $(D+h)=2.845$ in., height of enclosing cone=2.845 in., and the maximum travel of the inner cone was 2 in. The capacitance between the cones was measured for various values of D (see fig. 2) and is given in figure 4. As D was increased by a given amount, h was, of course, decreased

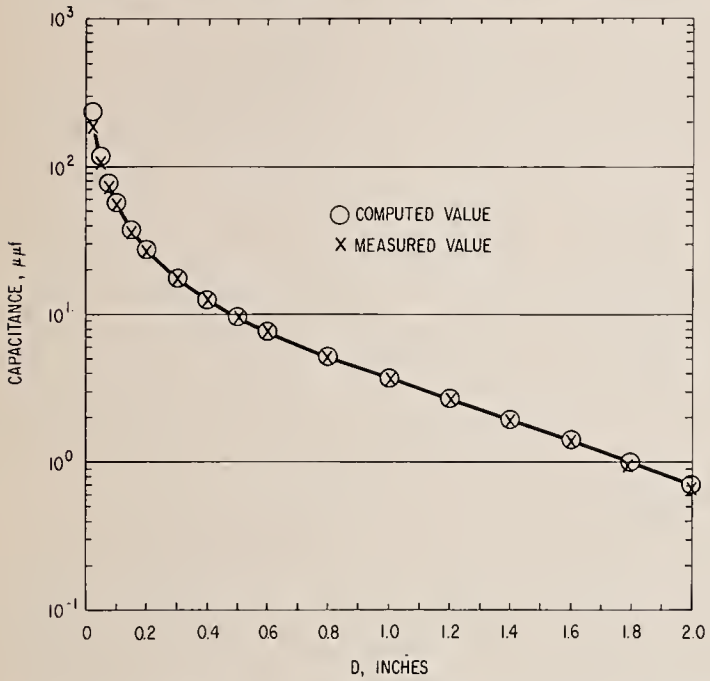

FIGURE 4. *Capacitance values of right-cone continuously adjustable capacitor versus displacement.*

by the same amount. The maximum value of D used was 2 in.; for this value of D there were still more than ¾ in. of the cones meshed; this helped reduce the end effects of the cones. Other steps to reduce this effect are described in the section below on precautions for measurement and application.

In order to compare the range of the conical capacitor with others, one must do so within the same mechanical precision limits, e.g., one must find the minimum value of D consistent with a reproducibility of say 0.2 percent in capacitance which is the precision considered above in the hypothetical cylindrical example. The derivative of C with respect to D or h will yield the necessary information.

The derivative is given in appendix II and results in

$$\frac{dC}{C}=\frac{dh}{h}[1+F(h)]$$

where

$$F(h)=-\frac{2(D+h)\cos^2\theta}{(h+2D\cos^2\theta)\left[\ln\left(1+2\frac{D}{h}\cos^2\theta\right)\right]} \tag{16}$$

The error in the capacitance is thus larger than that in h by the factor $[1+F(h)]$.

It is readily seen that $F(h)$ is a pure numeric, so that h and D may be stated in any consistent units. The table below gives some computed values of $F(h)$ and expeeted errors for the capacitor of figure 4 for

$$\frac{\Delta h}{h}\cong\frac{1}{3}\times10^{-4}:$$

This value of $\Delta h/h$ follows from the fact that at minimum spacing ($D=0.050$ in.) where $h=2.795$ a reproducibility of setting of 0.0001 in. is desired.

D	h	$F(h)$	$\Delta C/C$	C max.	C min.	$\frac{C\text{ max.}}{C\text{ min.}}$
in.	*in.*		%			
0. 050	2. 795	56	0. 2	116. 1	0. 69	168
. 100	2. 745	28	. 1	----------	----------	----------
. 500	2. 345	5	. 03	----------	----------	----------

626343—62——2

It appears, therefore, that for a resetability of h to 0.1 percent, reproducibility of capacitance values to 0.2 percent, and a maximum displacement of 2 in., the range of the conical capacitor of the above dimensions would be about 168 to 1, as against 40 to 1 for the cylindrical and 10 to 1 for the disk type. The conical capacitor recently found practical application at NBS in an attenuator-thermoelectric (AT) rf voltmeter for voltages from an average of 5 to 1,000 v at frequencies of 1 to 10 Mc/s [3].

As was observed above the heights of the cones were chosen to be close to 3 in. as compared to a maximum displacement of the 2 in. in order to reduce distortion of the electric field between the cones. A similar precaution for cylindrical electrodes would further reduce the capacitance range by a considerable amount depending on the diameter ratios of the two cylinders.

Figure 4 shows satisfactory agreement between computed and measured capacitance values of an experimental conical capacitor. The agreement was within ± 0.5 percent for all values of D to 1.6 in. For lower displacements the measured values are getting increasingly lower; the discrepancy is about 10 percent, for $D=0.05$ in., apparently as a result of limited accuracy in measuring true cone heights as well as limited mechanical perfection. Validity of formula (15) was also established for $\theta=20°$ and 45° with good agreement between computed and measured values.

4. Multiple Cone and Modified Shape Electrodes

Several female and male conical conductors may be combined to form respective electrodes of a single adjustable capacitor. Such a capacitor having three pairs of conductors is shown in figure 5. The advantage of this structure is that it renders capacitance values

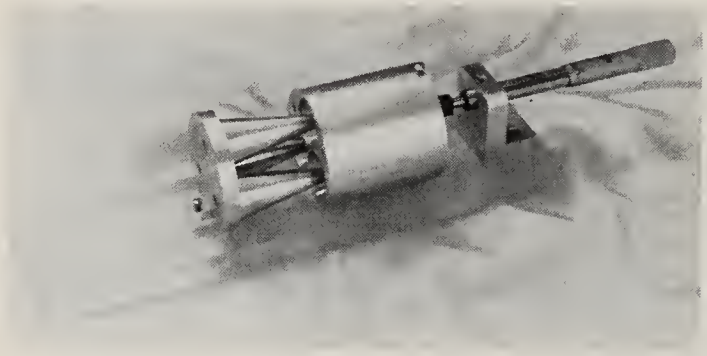

FIGURE 5. *Coaxial conical capacitor employing three pairs of cones.*

essentially equal to the values of a single pair times the number of pairs for the same available cylindrical space. In the example cited above the value of the conical angle may be doubled. This would require a shielding tube of about twice the original diameter. Yet the values of the new capacitance, as may be computed using eq (15), will increase by a negligible amount over the previous. However, one may place three pairs of cones of the original dimensions in the new shielding tube with a resultant capacitance three times the original values for each setting of the traveling electrode. The conclusion is that by means of multiple-cone electrodes one may obtain continuous coaxial capacitance ranges of say 1 to 150, or 2 to 300, or 3 to 450, etc., pf within practical space limitations. Moreover, longitudinal displacements of high accuracy at large values of D are relatively easy to obtain; this enables the realization of still larger capacitance ranges by reducing, say, the 3 pf capacity to 1 pf. Extrapolation of the curve of figure 4 shows that for dimensions equivalent to the constructed model a three-cone assembly plus an additional ½-in. displacement would increase the range by about two to one and would thus furnish an overall range of capacitance of about 300 to 1 without sacrifice in accuracy.

It is evident that one can obtain different curves of capacitance versus displacement by changing the cross-sectional contour of one or both surfaces of the electrodes from conical to other suitable shapes. This may be accomplished without affecting the overall range or ratio of maximum to minimum capacitances obtained with conical shapes. One should even

be able to increase the range further by making use of additional ring-flanges at the bases of the cones; the cross-sectional contours of these rings may in turn be shaped to produce a certain desired function of capacitance versus displacement. The idea is akin to the well-known shaping of the plates of variable air capacitors to obtain various responses, e.g., linear capacitance, linear frequency, linear wavelength, etc. The graphical field mapping method described in appendix III may be of assistance in the design of such capacitors.

5. Appendix I. Derivation of Equation (13) From Equation (12)

Referring to figure 2

$$r_a=(h+r_a \sin\theta) \sin\theta=h \sin\theta+r_a \sin^2\theta \tag{17}$$

$$r_b=(D+h+r_a \sin\theta) \sin\theta \tag{18}$$

or

$$r_a=\frac{h \sin\theta}{\cos^2\theta} \tag{19}$$

and

$$r_b=\left(D+h+h\frac{\sin^2\theta}{\cos^2\theta}\right)\sin\theta=[D\cos^2\theta+h(\cos^2\theta+\sin^2\theta)]\frac{\sin\theta}{\cos^2\theta}=(D\cos^2\theta+h)\frac{\sin\theta}{\cos^2\theta}. \tag{20}$$

Substituting into the denominator of eq (12) the values of r_a and r_b expressed in terms of D and h, we have

$$\ln\frac{2r_b\cos\theta-l\sin\theta}{2r_a\cos\theta-l\sin\theta}=\ln\frac{2(D\cos^2\theta+h)\frac{\sin\theta}{\cos^2\theta}\cos\theta-l\sin\theta}{2\frac{h\sin\theta}{\cos^2\theta}\cos\theta-l\sin\theta}=\ln\frac{2(D\cos^2\theta+h)-l\cos\theta}{2h-l\cos\theta}$$

$$=\ln\frac{2D\cos^2\theta+(2h-l\cos\theta)}{2h-l\cos\theta}=\ln\left[1+\frac{2D\cos^2\theta}{2h-l\cos\theta}\right]. \tag{21}$$

Therefore

$$C=\frac{2\pi\epsilon l\cos\theta}{\ln\left[1+\frac{2D\cos^2\theta}{2h-l\cos\theta}\right]} \tag{22}$$

which is the same as eq (13) above.

6. Appendix II. Derivation of Equation (16)

Starting with eq (14)

$$C=\frac{2\pi\epsilon h}{\ln[1+2(D/h)\cos^2\theta]}$$

Let $D+h$=height of outside cone=a constant=H.

Let $2\pi\epsilon=K_1$ and $2\cos^2\theta=K_2$. Then, $D=H-h$ and

$$\frac{1}{K_1}C=h\left[\ln\left(1+K_2\frac{H-h}{h}\right)\right]^{-1} \tag{23}$$

$$\frac{1}{K_2}\frac{dC}{dh}=\left[\ln\left(1+K_2\frac{H-h}{h}\right)\right]^{-1}$$

$$-h\left[\ln\left(1+K_2\frac{H-h}{h}\right)\right]^{-2}\cdot\frac{1}{\left[1+K_2\frac{H-h}{h}\right]}\cdot K_2\left(-\frac{H}{h^2}\right) \tag{24}$$

$$=\left[\ln\left(1+K_2\frac{H-h}{h}\right)\right]^{-1}+\left[\ln\left(1+K_2\frac{H-h}{h}\right)\right]^{-2}\frac{K_2H}{\left(1+K_2\frac{H-h}{h}\right)h} \tag{25}$$

$$=\left[\ln\left(1+K_2\frac{H-h}{h}\right)\right]^{-1}\left\{1+\frac{K_2H}{\left(1+K_2\frac{H-h}{h}\right)h\left[\ln\left(1+K_2\frac{H-h}{h}\right)\right]}\right\} \tag{26}$$

$$=\left[\ln\left(HK_2\frac{H-h}{h}\right)\right]^{-1}\left\{1+\frac{K_2H}{[h+K_2(H-h)]\left[\ln\left(1+K_2\frac{H-h}{h}\right)\right]}\right\} \tag{27}$$

but

$$\left[\ln\left(1+K_2\frac{H-h}{h}\right)\right]^{-1}=\frac{C}{K_1h}\therefore\frac{1}{K_1}\frac{dC}{dh}=\frac{C}{K_1h}\left\{1+\frac{K_2H}{[h+K_2(H-h)]\left[\ln\left(1+K_2\frac{H-h}{h}\right)\right]}\right\} \tag{28}$$

and

$$\frac{dC}{C}=\frac{dh}{h}\left\{1+\frac{K_2H}{(h+K_2D)\left[\ln\left(1+K_2\frac{D}{h}\right)\right]}\right\} \tag{29}$$

or

$$\frac{dC}{C}=\frac{dh}{h}\left\{1+\frac{2H\cos^2\theta}{(h+2D\cos^2\theta)\left[\ln\left(1+2\frac{D}{h}\cos^2\theta\right)\right]}\right\}. \tag{30}$$

The interpretation of eq (30) is that the error in C is equal to the error in h plus another multiple of that error in h. This multiple is expressed by the second term of (30); namely, by

$$F_{(h)}=\frac{2(D+h)\cos^2\theta}{(h+2D\cos^2\theta)\left[\ln\left(1+2\frac{D}{h}\cos^2\theta\right)\right]} \tag{31}$$

which is also given in eq (16) above.

7. Appendix III. Graphical Field Mapping

Maps showing the distribution of the equipotential surfaces and electric flux lines provide a tool to compute the capacitance between electrodes of any shape. The principle is based on subdividing the space between the electrodes into local-equal-capacitance cells [4, 5, 6]. These cells are counted and are combined in series-parallel arrangements yielding the total capacitance between the electrodes. The simplest case is that of "two-dimensional fields" to which the method has been applied widely for many years. The field in this case is represented by means of "curvilinear squares" in one cross-sectional plane and is identical to the field in all other planes parallel to it. The lines of force lie within these planes. Figure 6 shows such a field confined between two wedge-shaped electrodes in a homogeneous isotropic dielectric. One might mistakenly assume that such a field distribution holds for the case of a conical capacitor. This is not so because here the field is not the same in any system of planes intersecting the cones parallel to their axis. Nor does the case of coaxial cylindrical electrodes

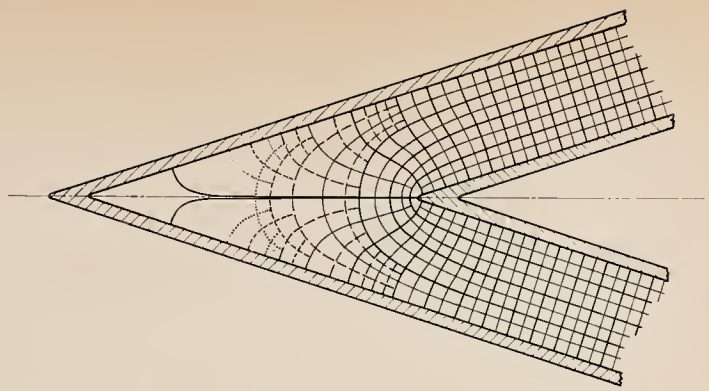

FIGURE 6. *Electric field map in a homogeneous isotropic dielectric of a parallel-side, wedge-shape capacitor.*

apply to cones beeause the system of planes perpendieular to the axis of the cylinders does not furnish the necessary conditions to describe a field; the lines of force intersect these planes at some angles, and the fields are not identical in all of these planes.

For coaxial eonical surfaces the "axial-symmetry field" is applieable. These fields are more complicated than the "curvilinear square" fields, but they still have a major advantage over the ease in whieh no type of symmetry exists, in that the fields may be represented in one plane. The "eells" are shown as "curvilinear rectangles." For the present purpose it will not be neeessary to count and sum up the cells. It will be suffieient to show that the potential gradient is essentially the same all along the surface of the inner cone. This is shown graphically in figure 3. As discussed in appendix IV, the assumption of uniform charge density and the integration leading to eq (13) are therefore justified. The case of relatively large displacement of the adjustable electrode was intentionally ehosen for this figure to show up field distortions better.

It is generally immaterial what procedure one follows in eonstructing a field map, as long as the final map meets certain tests. The tests for this case are stated below. One may use a trial and error proeedure from start to finish. Or one may use short cuts by means of approximate computations; the approximate positions of the curves are then readjusted by trial and error to satisfy the test requirements as best as possible. This latter short-cut approaeh was applicable here.

The field construction steps were briefly as follows. A field in a space having axial symmetry may be subdivided into cells having equal "local" capacitance values δC where

$$\delta C = 2\pi\epsilon \frac{\rho \delta s}{\delta l}; \tag{32}$$

ρ is the effeetive distance of the cell from the axis, i.e., its radius of rotation, δs and δl are orthogonal curvilinear line elements forming the "rectangle," δl is the distanee between the side representing two equipotential surfaces, δs is the distanee representing the width of a "tube of flux" and ϵ is the dielectric constant. The cell is thus a ring having an effective radius ρ and a eross section of $\delta s \cdot \delta l$.

It follows that in order for the cells to have the same capacitanee either δs or δl must be varied as ρ varies. In case of a coaxial line, the distance from the axis of rotation increases at a given point along the axis, ρ inereases, δs is kept eonstant, and δl is made to be directly proportional to ρ. From the geometry of a eoaxial right cireular eonical capacitor with relatively small apex angles the location of the equipotential surface whose potential is midway between the potential of the two cones is given approximately by the four equations given below It follows from the above that

$$\delta l_1 + \delta l_2 = T = \text{eonstant dimension of a ring along the radius}$$

$$\frac{\rho_1}{\delta l_1} \text{ must} = \frac{\rho_2}{\delta l_2}.$$

For small values of θ,

$$\frac{\rho_a}{\rho_1}=2\,\frac{\rho_1}{1/2T+\rho_1}-\frac{\rho_a}{1/2T+\rho_1}.$$

$$4\rho_1^2-4\rho_a\rho_1-T\rho_a=0.$$

Therefore

$$\rho_1\cong\frac{1}{2}\,\rho_a+\sqrt{\left(\frac{\rho_a}{2}\right)^2+\frac{T\rho_a}{4}} \tag{33}$$

$$\rho_2\cong 1/2T+\rho_1 \tag{34}$$

$$\delta l_1\cong 2(\rho_1-\rho_a) \tag{35}$$

$$\delta l_2\cong T-\delta l_1. \tag{36}$$

Here ρ_a is the radius of rotation of the inner cone at the chosen point along the axis and T is the constant distance between the electrodes measured along that radius; only the positive value of ρ is used, ρ_1 is the radius of the center of the cell closer to the axis. ρ_2 is the approximate radius of the center of the second cell, farther from the axis, δl_1 is the approximate distance between the inner cone and the new equipotential plane, δl_2 is the distance between the outer cone and the new equipotential plane.

One must check the results by seeing that

$$\frac{\rho_1}{\delta l_1}=\frac{\rho_2}{\delta l_2}. \tag{37}$$

Any other approximate equipotential-line position corresponding to the above given location along the axis may be found in a similar manner; one may consider the new equipotential line determined above as the surface of the inner (or outer) cone and split the rest of the upper (or lower) space into two effective cell layers, thus rendering positions for surfaces having ¼ (or ¾) of the potential-difference given. Choosing several positions along the axis, one may plot the sections of equipotential planes with the plane of the paper.

Having approximately located the equipotential lines one must next locate the "flux tube" boundaries for equal cells. These are fixed by the values of δ's which should in our case vary inversely proportional to ρ as one travels along the axis of symmetry.

The test of the accuracy of the finished plot is in its satisfying the following conditions: (1) The field lines must be orthogonal, (2) the flux lines as well as the flux-tube boundaries must be normal to the conductor surfaces, and (3) the "rectangles" having the same value of ρ must be similar. The position of the field lines are, therefore, adjusted by trial and error to satisfy this test. The above conditions seem to be met in the plot of figure 3 to a sufficient accuracy.

8. Appendix IV. Justifications of Basic Assumption for Approximate Solution

The approximate expression (13) was derived on the assumption that the equipotential surfaces are everywhere parallel. Figure 3 shows these surfaces departing from parallelism by a noticeable amount; as a result, one would at a first glance expect a considerable disagreement between experimental and computed data. The following reasons may explain why no appreciable discrepancy was observed at the measurement accuracies quoted.

The basis of the assumption that the charge distribution over the conical surfaces is essentially uniform is a physical visualization of two closely spaced parallel conducting closed surfaces of any shape. If one assumes a certain potential of the inner conductor and zero potential on the outer (shield), the charge distribution over the inner will be a normal function of the contour when the spacing between these conductors is infinity. As this spacing is reduced to zero the surface charges will approach uniformity.

At relatively small spacings, uniform charge distribution may be assumed with fairly good accuracy.

Maxwell, Howe, Schelkunoff, and Friis [7, 8, 9], and others have shown that fairly accurate capacitance evaluations result from assuming uniform charge distribution even for simple, unshielded conductors. If one assumes uniform charge distribution over a particular conductor of a system, its average potential will be closely equal to the uniform potential it attains when the same total charge has its natural distribution. Howe has shown that an error less than 1 percent in capacitance results from assuming uniform charge distribution on a long straight wire in free space. Maxwell and others have shown that first-order errors in the assumed charge distribution lead only to second-order errors in capacitance.

An additional justification may be found in the fact that the relative potential distribution in our case is changing with displacement; the departure from parallelism, and hence the error, will increase with the value of $(r_b - r_a)$. It will also increase for increased conical angles and with increased ratios of $(r_b - r_a)/h$. Since the conical angles as well as the ratios of $(r_b - r_a)/h$ over most of the range in the present case were relatively small, this may account for a further reduction in the expected discrepancy.

9. Appendix V. Precautions for Measurement and Application

Though the precautions to be taken during measurement and applications of conical capacitors are obvious, it may be worthwhile to mention some of these here.

Since either the male or the female cones may be chosen as the traveling electrode, one must watch out for the effect of the stray capacitance from the male to the surrounding objects and ground.

For measurement purposes it is best to ground the male and to do it in such a way that the grounding leads are always kept as far as possible away from the female (outer) cone. The male cone should be mounted on an insulating base placed at the largest diameter of the male. The female-cone rim (or wall) thickness should be kept at a minimum in order to reduce fringing flux. To still further reduce this fringing flux it is advisable to place a guard band closely around the opening of the female cone; this band should be insulated from the female and should be grounded. To obtain true increments of individual cones of multiple cone units it may be best to start with the well assembled complete unit first and then remove one male at a time.

In applications one must keep in mind the input impedance variation of the male to ground. The male cone is usually the grounded traveling electrode. In case of the AT voltmeter [3], for example, the use of the male as the high-potential constant input impedance electrode is necessary. Where application requires it, one may add flanges or rings at the bases of the conical electrodes to increase the maximum capacity and range of this type of capacitor still further. One may also design contour shapes other than conical in order to obtain various functions of capacitance increments versus displacement similar to the various shapes (linear frequency, linear capacitance, linear wavelength, etc.) used with variable parallel-plate air capacitors.

10. Appendix VI. Rigorous Solution of Problem

A solution is understood to be "rigorous" when no approximations are made in any of the steps of its derivation from a basic differential equation and when this solution is expressed in a finite number of terms or in a convergent series of terms with the general term precisely known. A rigorous solution must satisfy the differential equation and boundary condition and must also be the only solution possible. The rigorous solution of a boundary value problem in electrostatic field distribution leading to the determination of capacitance between electrodes, requires the following steps:

1. Selection of coordinate system,
2. expression of Laplace's equation in this system,
3. general solution of this equation,

4. application of boundary values and determination of constants to obtain a solution for the potential distribution of the particular problem at hand.
5. the steps mentioned previously leading from a known potential distribution to capacitance.

The criteria for choosing a coordinate system are the difficulties anticipated in steps 3 and 4. Stratton [10] concluded that the only practical general procedure to solve Laplace's equation is to employ a set of orthogonal curvilinear coordinates and the method of separation of variables or "product solution".

As was discussed above under field construction, a three-dimensional coordinate system must be used in this case despite the symmetry about the common axis of the cones [11].

The potential at any point in space is in this approach equal to the product of independent functions, say, $R\theta\Phi$, where R is a function of the radius vector alone, θ of one of the coordinate angles alone, and Φ of the other coordinate angles alone. Prescribed boundaries should coincide with surfaces of the families of the coordinates. Oblique systems of coordinates, though of greatest practical importance, unfortunately lead to partial differential equations which cannot be solved as yet. Material on this subject, written at later dates [12, 13, 14, 15] does not seem to shed further light on the subject nor does it offer a practical way of handling a problem like the present where an oblique system seems to be the most suitable. This later system should preferably consist of right conical surfaces, spherical surfaces and planes; the apexes of the cones should move along the z axis. Figure 7 shows the coordinates of this system.

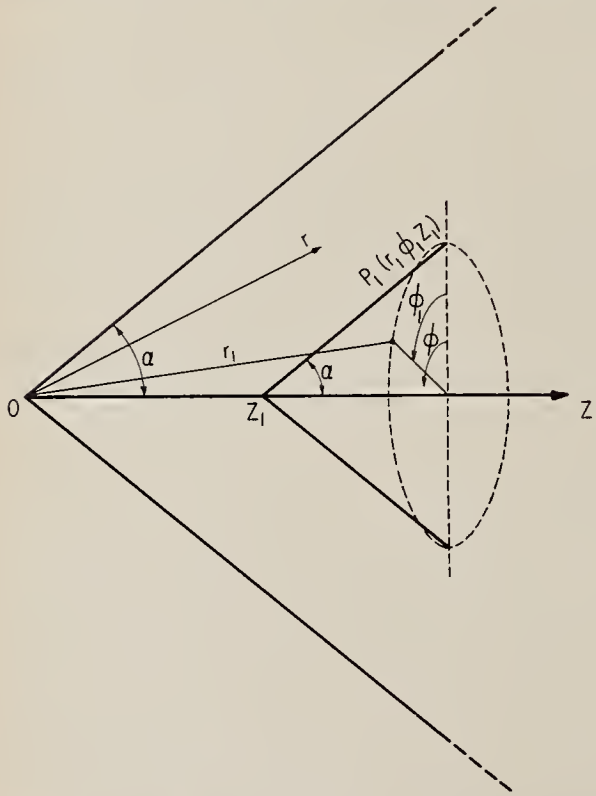

FIGURE 7. *Oblique three-dimensional conical coordinate system.*

α is a constant solid angle. Coordinates r, ϕ, z fix location of point P; $z=z_1$ renders a family of parallel coaxial conical surfaces; $r=r_1$, a family of concentric spherical surfaces; and $\phi H\phi_1$, a family of planes through axis z.

Several texts [16, 17, 18] have treated the conical case and, unfortunately, limited the analysis to systems of cones having a single apex. The method of images is widely used in cases of point and line charges; however it is impractical for more complex cases like the present. The method of superposition of fields produced individually inside one cone and outside another cannot be used because of the inevitable interaction effect which cannot possibly be neglected when the cones are brought closer to each other.

A promising approach to the present case in orthogonal coordinates seems to be the application of the series expansion solution [19, 20, 21, 22, 23, 24]. This approach requires that at a fixed, finite value of one of the functions of, say, $V=R\theta$ (e.g., for $R=R_1\neq 0$ and $R_1\neq\infty$) the value of the other should result in an expandable series, say, $V_1=R_1\theta$ where θ is an expandable function in terms of Fourier trigonometric or Legendre series. The constants of the terms

can then be found; R_1 is a factor incorporated in these constants and may be treated as a variable parameter of the final solution. The value of R_1 is arbitrary; the only requirement is that it be much larger than D. The particular value of R_1 chosen will affect the accuracy of the solution; to this extent the solution ceases to be "rigorous". Once determined for the boundary surface where $V=V_1$, these constants are put into the general solution which thus renders the value of V for all values of r. These steps may be specifically outlined as follows.

The general solution of Laplace's equation in polar spherical coordinates for the case of axial symmetry is [25, 26]

$$V=\sum_{n=0}^{\infty}(A_n r^n+B_n r^{-n-1})[C_n^1 P_n(\cos\theta)K_n^1 Q_n(\cos\theta)] \tag{38}$$

where A_n, B_n, C_n^1, and K_n^1 are constants, $P_n(\cos\theta)$ and $Q_n(\cos\theta)$ are Legendre coefficients of first and second kind, respectively. For $\theta=0$, $Q_n=\infty$. Therefore, the terms containing Q_n will remain in the solution for all values of $r>D$, where the space excludes the $\theta=0$ region from the solution (see fig. 8a), and will drop out for $r<D$ because V cannot reach infinity anyplace. In general, terms containing the Legendre coefficients of the second kind (second kind zonal harmonics), Q_n, drop out from solutions where the space boundaries of the voltage distribution to be determined, include the axis of symmetry. On the other hand if this space is everywhere away from the axis (i.e., for $\theta\neq 0$), these terms remain in the solution. It would thus normally be necessary to apply two solutions to the case in question, one for $r>D$ and the other for $r<D$; for $r=D$ either solution should apply.

Because V cannot be infinite A_n must equal zero, otherwise for $r=\infty$, V would be$=\infty$. One can also combine the constants and make $B_nC_n^1=C_n$ and $B_nK_n^1=K_n$.

The solution for $r>D$ thus reduces to

$$V=\sum_{n=0}^{\infty} r^{-n-1}[C_nP_n(\cos\theta)+K_nQ_n(\cos\theta)]. \tag{39}$$

The solution for $r<D$ may be in this case neglected as it is of minor importance and amounts only to a correction caused by fringing flux. It could, however, be treated in a similar manner as the rest of the field.

A glance at figure 8a will reveal that for $r>>D$ the shape of the function of V versus θ

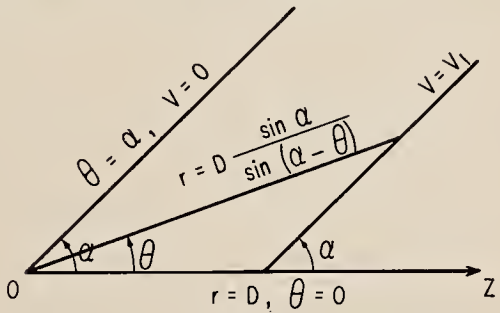

(a)

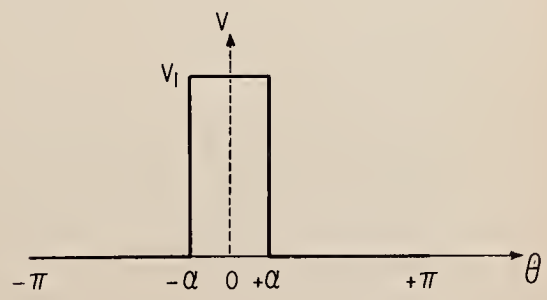

(b)

FIGURE 8. (a) *Polar spherical coordinate system* r, θ, ϕ; $\theta=0$ *is an axis of symmetry;* (b) *Potential distribution function for* r≫D.

will be similar to a rectangular pulse. One can assign a value $r=r_1$ (say, $r_1=100D$ or $1000D$) for which the pulse is rectangular to any accuracy desired. The width of the pulse is 2α, the period is 2π and its amplitude is V_1. Figure 8b shows one cycle of this function, between $-\pi$ and $+\pi$. Such a restricted piecewise continuous function can be expanded in the interval $(-\pi, \pi)$ in a series of Legendre polynomials in the form of [20, 21, 24, 27, 28, 29]

$$F(\cos\theta)=\sum_{n=0}^{\infty} C_n P_n(\cos\theta) \tag{40}$$

where the coefficients C_n are given by

$$C_n=\frac{2n+1}{2}\int_{-\pi}^{\pi} F(\theta)P_n(\cos\theta)\sin\theta d\theta. \tag{41}$$

The solution is expressed in (39) in terms of Legendre functions of both first and second kind. In order to attempt a series expansion it seems best to express this solution in terms of the first kind only, using the interrelation between the two shown, for example, by Smythe [30] in an alternate general solution as

$$\theta=A_n^1 P_n(\mu)+B_n\left[1/2P_n(\mu)\ln\frac{\mu+1}{\mu-1}-\frac{2n-1}{1\cdot n}P_{n-1}(\mu)-\ \ldots\right] \tag{42}$$

or

$$\theta=\left[A_n^1+B_n\frac{1}{2}\ln\frac{\mu+1}{\mu-1}\right]P_n(\mu)-B\frac{2n-1}{1\cdot n}P_{(n-1)}(\mu)-\ \ldots \text{ here } \mu=\cos\theta. \tag{43}$$

The general solution is then

$$V=\sum_{n=0}^{\infty} r^{-n-1}\left[\left(A_n^1+B_n\frac{1}{2}\ln\frac{\mu+1}{\mu-1}\right)P_n(\mu)-B\frac{2n-1}{1\cdot n}P_{(n-1)}(\mu)-\ \ldots\right]. \tag{44}$$

The solution of the problem depends thus on the prospects of having (44) developed into a Fourier-Legendre-series. Once such a series could be obtained the next steps, as indicated above, would be to (1) find the constants of this series from figure 8b, (2) substitute $r=r_1$, and $V=V_1$, into (44), and (3) equate the two series term by term to find the coefficients for the solution (44).

No development of (44) into a Fourier-Legendre [31] series seems to be available at present. The presence of the term $\ln\frac{\mu+1}{\mu-1}$ and of an additional constant factor for the term $P_n(\mu)$ makes such an approach doubtful, despite the fact that figure 8b strongly supports it.

11. References

[1] J. C. Balsbaugh and P. H. Moon, A bridge for precision power-factor—measurements on small oil samples, Trans. AIEE **52,** 528–536 (June 1933).

[2] Leigh Page, Introduction to Theroretical Physics, chapter 10, (D. Van Nostrand Co., Inc., Princeton, N.J., 1935). F. W. Sears, Electricity and Magnetism, chapters 1, 2, and 3 (Addison-Wesley Publishing Co., Inc., Reading, Mass., 1954).

[3] These types of voltmeters were announced and briefly described in NBS Tech. News Bul. **40,** 29–30 (1956).

[4] A. D. Moore, Fundamentals of Electrical Design, p. 61 (McGraw-Hill Book Co., Inc., New York, N.Y., 1927).

[5] S. S. Attwood, Electric and Magnetic Fields, pp. 62–69, 74–75, 174–175 (John Wiley and Sons, Inc., New York, N.Y., 2d ed., 1941).

[6] E. Weber, Electro-Magnetic Fields, vol. 1, pp. 197–204 (John Wiley and Sons, Inc., New York, N.Y., 1950). Additional references are listed on pp. 204 and 205.

[7] J. C. Maxwell, A Treatise of Electricity and Magnetism, vol. 1, pp. 148–154 (Oxford University Press, New York, N.Y., 1904).

[8] S. A. Schelkunoff and H. T. Friis, Antennas Theory and Practice, pp. 313–317 (John Wiley and Sons, Inc., New York, N.Y., 1952).

[9] G. W. O. Howe, The calculation of aerial capacitances, Wireless Eng. **20,** 157–158 (1943). The capacity of an inverted cone and the distribution of its charge, Proc. Phys. Soc. (London, England), **29,** 339–344 (1917).
[10] J. M. Stratton, Electro-Magnetic Theory, pp. 47–51, 194–197 (McGraw-Hill Book Co., Inc., New York, N.Y., 1941).
[11] W. R. Smythe, Static and Dynamic Electricity, p. 111 (McGraw-Hill Book Co., Inc., New York, N.Y., 1950).
[12] Smythe, ibid., pp. 50–95, 133–155.
[13] S. Ramo and J. R. Whinnery, Fields and Waves in Modern Radio, pp. 145, 173–174 (John Wiley and Sons, Inc., New York, N.Y., 1953).
[14] Stratton, op. cit., pp. 47, 197.
[15] S. A. Schelkunoff, Applied Mathematics for Engineers and Scientists, pp. 138–160, 417–427 (D. Van Nostrand Co., Inc., Princeton, N.J., 1948).
[16] Smythe, op. cit., p. 146.
[17] Weber, op. cit., pp. 493–495.
[18] W. E. Beyerly, An Elementary Treatise on Fourier Series and Spherical, Cylindrical, and Ellipsoidal Harmonics, pp. 191–194 (Ginn and Co., Boston, Mass., 1893).
[19] Ramo and Whinnery, op. cit., pp. 171–176.
[20] I. S. Sokolnikoff, Higher Mathematics for Engineers and Physicists, pp. 342–386 (McGraw-Hill Book Co., Inc., New York, N.Y., 1941).
[21] W. Kaplan, Advanced Calculus, pp. 425–427 (Addison-Wesley Publishing Co., Inc., Reading, Mass., 1953).
[22] Smythe, loc. cit.
[23] R. V. Churchill, Fourier Series and Boundary Value Problems, pp. 175–178 (McGraw-Hill Book Co., Inc., New York, N.Y., 1941).
[24] W. C. Johnson, Mathematical and Physical Principles of Engineering Analysis, pp. 242–245 (McGraw-Hill Book Co., Inc., New York, N.Y., 1944).
[25] Smythe, op. cit., pp. 129, 143.
[26] J. C. Slater and N. H. Frank, Introduction to Theoretical Physics, pp. 202–203 (McGraw-Hill Book Co., Inc., New York, N.Y., 1933).
[27] J. H. Jeans, Mathematical Theory of Electricity and Magnetism, p. 223 (Cambridge University Press, New York, N.Y., 1925).
[28] T. M. MacRobert, Spherical Harmonics, pp. 95–96, 102–103 (Dover Publications, Inc., New York, N.Y., 2d edition, 1948).
[29] Beyerly, op. cit., p. 170.
[30] Smythe, op. cit., p. 145.
[31] Among the references consulted for such a development were also: E. W. Hobson, Spherical and Ellipsoidal Harmonics (Chelsea Publishing Co., New York, N.Y., 1931), according to Smythe (op. cit., p. 217, 1939 and 1950) "includes almost everything known about the subject."
P. Franklin, Methods of Advanced Calculus, chapter XI (McGraw-Hill Book Co., Inc., New York, N.Y., 1944).
J. D. Kraus, Electromagnetics, pp. 519–541 (McGraw-Hill Book Co., Inc., New York, N.Y., 1953).
F. D. Murnaghan, Introduction to Applied Mathematics, pp. 166–174 (John Wiley and Sons, Inc., New York, N.Y., 1948).
E. T. Whittaker and G. N. Watson, A Course of Modern Analysis, pp. 303–323 (Cambridge University Press, New York, N.Y., 1952).

U.S. GOVERNMENT PRINTING OFFICE: 1962

U.S. DEPARTMENT OF COMMERCE
Luther H. Hodges, *Secretary*

NATIONAL BUREAU OF STANDARDS
A. V. Astin, *Director*

THE NATIONAL BUREAU OF STANDARDS

The scope of activities of the National Bureau of Standards at its major laboratories in Washington, D.C., and Boulder, Colorado, is suggested in the following listing of the divisions and sections engaged in technical work. In general, each section carries out specialized research, development, and engineering in the field indicated by its title. A brief description of the activities, and of the resultant publications, appears on the inside of the front cover.

WASHINGTON, D.C.

Electricity. Resistance and Reactance. Electrochemistry. Electrical Instruments. Magnetic Measurements. Dielectrics. High Voltage.
Metrology. Photometry and Colorimetry. Refractometry. Photographic Research. Length. Engineering Metrology. Mass and Scale. Volumetry and Densimetry.
Heat. Temperature Physics. Heat Measurements. Cryogenic Physics. Equation of State. Statistical Physics.
Radiation Physics. X-ray. Radioactivity. Radiation Theory. High Energy Radiation. Radiological Equipment. Nucleonic Instrumentation. Neutron Physics.
Analytical and Inorganic Chemistry. Pure Substances. Spectrochemistry. Solution Chemistry. Standard Reference Materials. Applied Analytical Research.
Mechanics. Sound. Pressure and Vacuum. Fluid Mechanics. Engineering Mechanics. Rheology. Combustion Controls.
Organic and Fibrous Materials. Rubber. Textiles. Paper. Leather. Testing and Specifications. Polymer Structure. Plastics. Dental Research.
Metallurgy. Engineering Metallurgy. Microscopy and Diffraction. Metal Reactions. Metal Physics. Electrolysis and Metal Deposition.
Mineral Products. Engineering Ceramics. Glass. Refractories. Enameled Metals. Crystal Growth. Physical Properties. Constitution and Microstructure.
Building Research. Structural Engineering. Fire Research. Mechanical Systems. Organic Building Materials. Codes and Safety Standards. Heat Transfer. Inorganic Building Materials.
Applied Mathematics. Numerical Analysis. Computation. Statistical Engineering. Mathematical Physics. Operations Research.
Data Processing Systems. Components and Techniques. Computer Technology. Measurements Automation. Engineering Applications. Systems Analysis.
Atomic Physics. Spectroscopy. Infrared Spectroscopy. Solid State Physics. Electron Physics. Atomic Physics.
Instrumentation. Engineering Electronics. Electron Devices. Electronic Instrumentation. Mechanical Instruments. Basic Instrumentation.
Physical Chemistry. Thermochemistry. Surface Chemistry. Organic Chemistry. Molecular Spectroscopy. Molecular Kinetics. Mass Spectrometry.

Office of Weights and Measures.

BOULDER, COLO.

Cryogenic Engineering. Cryogenic Equipment. Cryogenic Processes. Properties of Materials. Cryogenic Technical Services.
Ionosphere Research and Propagation. Low Frequency and Very Low Frequency Research. Ionosphere Research. Prediction Services. Sun-Earth Relationships. Field Engineering. Radio Warning Services. Vertical Soundings Research.
Radio Propagation Engineering. Data Reduction Instrumentation. Radio Noise. Tropospheric Measurements. Tropospheric Analysis. Propagation-Terrain Effects. Radio-Meteorology. Lower Atmosphere Physics.
Radio Standards. High Frequency Electrical Standards. Radio Broadcast Service. Radio and Microwave Materials. Atomic Frequency and Time Interval Standards. Electronic Calibration Center. Millimeter-Wave Research. Microwave Circuit Standards.
Radio Systems. Applied Electromagnetic Theory. High Frequency and Very High Frequency Research. Modulation Research. Antenna Research. Navigation Systems.
Upper Atmosphere and Space Physics. Upper Atmosphere and Plasma Physics. Ionosphere and Exosphere Scatter. Airglow and Aurora. Ionospheric Radio Astronomy.